Dynamic Analysis of Heterogeneous Azeotropic Distillation

Soemantri Widagdo
Dept. of Chemistry & Chemical Engineering, Stevens Institute of Technology, Hoboken, NJ 07030

Warren D. Seider
Dept. of Chemical Engineering, University of Pennsylvania, Philadelphia, PA 19104

Donald H. Sebastian
Dept. of Chemistry & Chemical Engineering, Stevens Institute of Technology, Hoboken, NJ 07030

A model and algorithm are presented for the separation of mixtures where the phase distribution on the trays is extremely uncertain, as it occurs when the mixtures have two partially-miscible binary pairs and a minimum-boiling ternary azeotrope. Included are an algorithm for the consistent initialization of index-1 differential/algebraic equations, a novel algorithm for branch switching when the phase distribution changes at a real bifurcation point, and a reliable algorithm for phase stability analysis. Open-loop responses are presented for the dehydration of secbutanol with disecbutylether in single-stage, 12-tray, and 33-tray separators. These simulation results for the 33-tray tower are in qualitative agreement with experimental measurements for the ARCO SBA-II tower.

Introduction

The steady-state behavior of heterogeneous azeotropic distillation towers has been studied extensively. Many algorithms for solving the MESH (material balance, equilibrium, summation of mole fractions, and heat balance) equations, with various strategies to calculate liquid-phase splitting, have been proposed (Block and Hegner, 1976; Ross and Seider, 1980; Ferraris and Morbidelli, 1981; Kovach and Seider, 1987a,b; Swartz and Stewart, 1987; Baden and Michelsen, 1987). Most of these algorithms have been tested for mixtures with one partially-miscible binary pair, usually the ethanol-benzene-water mixture.

Kovach and Seider (1987a,b) reported experimental measurements and simulated the ARCO SBA-II tower for the dehydration of secbutanol (SBA) with disecbutylether (DSBE) as the entrainer. The SBA-DSBE-water system was the first to have two partially-miscible binary pairs, with a very small VLLE region on the top tray, at temperatures approaching the low-boiling, heterogeneous ternary azeotrope. The great sensitivity of its phase diagram to small changes in composition, temperature and pressure is shown in our companion article (Widagdo et al., 1992) and briefly reviewed herein. This sensitivity establishes the importance of determining the phase distribution accurately for systems such as these.

Kovach and Seider (1987a,b) were the first to calculate two liquid phases far into the stripping section, with a temperature front at the interface between trays having one and two liquid phase(s) that matches the experimental measurements. In a laboratory tower, Cairns and Furzer (1990) reported similar behavior for a mixture of ten hydrocarbons and water. These temperature and concentration fronts are steep and their position, at the interface between trays having one and two liquid phase(s), is highly sensitive to the aqueous reflux (Kovach and Seider, 1987a,b; Widagdo et al., 1989). These towers are also characterized by multiple solutions of the steady-state MESH equations (Kovach and Seider, 1987a,b; Widagdo et al., 1989).

To avoid operability and control problems, large numbers of trays have been installed, often far in excess of those required to achieve the separation, partially because reliable models have been slow to develop. This is confirmed by the simulations of Widagdo et al. (1989), which indicate that the trays in the SBA-II tower can be reduced by two-thirds while maintaining a high purity and recovery of secbutanol. This observation

Correspondence concerning this article should be addressed to W. D. Seider.

and the experimental measurements of Herron et al. (1988) who demonstrate, contrary to the common belief, that the second liquid phase has no significant effect on the tray hydraulics and efficiency, strongly support the contention that more costly designs, intended to avoid two liquid phases on the trays, are unnecessary.

For these towers, the bottoms product purity is commonly controlled indirectly by measuring the difference between the temperature on two trays in the stripping section and by manipulating the aqueous reflux rate. In the SBA-II tower the bottoms purity is controlled manually, probably because of a reluctance to trust automatic controllers to monitor such a sensitive process. Furthermore, if these towers were built with substantially fewer trays, the response to disturbances would be more difficult to monitor. Some kind of automatic control strategy, preferably based on a rigorous dynamic model, would seem necessary to reduce the cost of these towers. Hence, an objective of this work has been to develop such a model to assess the controllability and operability of shortened towers. Its development, however, has not been easy, primarily because liquid-phase splits at real bifurcation points must be calculated accurately and singularities in the *differential/algebraic* systems must be avoided.

Recently, Rovaglio and Doherty (1990) presented a model that tracks the movement of the L-LL interface in time. The dynamics of a tower for the dehydration of ethanol with benzene were simulated under conditions where three or more steady-state solutions are exhibited. In response to a 10% increase in the feed flow rate, the tower shifts from steady operation through an intermediate, unstable steady state to a third steady state. Their results focus on the steady-state attractors, rather than the dynamic response.

Wong et al. (1991) extended the Ballard and Brosilow (1978) formulation, which was used by Prokopakis and Seider (1983), to model the changes in the phase distribution when dehydrating ethanol with benzene. Dynamic responses to changes in the feed flow rate and composition, aqueous reflux ratio, reboiler duty, and entrainer makeup rate are studied. A PI controller is proposed to control the purity of ethanol in the bottoms product by measuring the temperature on a tray in the stripping section and manipulating the aqueous reflux rate.

Despite this progress, for many towers more reliable methods are needed to track the interface between trays having one and two liquid phase(s). This study concentrates on the necessary conditions to provide an index-1 formulation, with consistent reinitialization and branch switching at a real bifurcation point, when the phase distribution changes on a tray. The methods developed herein are used to simulate the dehydration of sec-butanol. The effects of changes in the feed flow rate, aqueous reflux ratio, aqueous reflux rate, and reboiler duty on the SBA-II tower and a shortened tower are studied.

Model Formulation

The model presented herein is a dynamic extension of the Naphtali-Sandholm (1971) formulation, also extended to model stages having two liquid phases. Consider a column with N_t trays that separates N_s species. The top stage, tray-1, represents the condenser and decanter combined. The bottom stage, tray-N_t, represents the reboiler. In the model, the vapor and liquid streams, leaving each tray, are assumed to be at equilibrium.

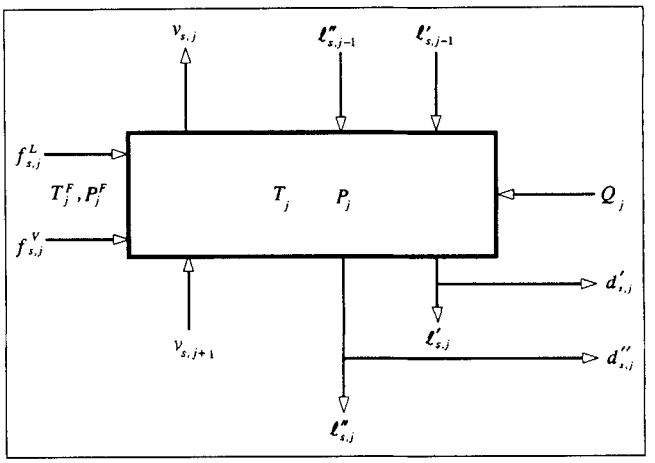

Figure 1. Equilibrium stage.

Two liquid phases, when they coexist, are vigorously mixed, and hence they are assumed to be at equilibrium. Note that LLE was confirmed by Herron et al. (1988), who measured the distribution of acetone between mineral oil and water in the presence of air on a sieve tray. Furthermore, each stage may have a feed stream and liquid side streams, and can exchange heat with the surroundings, as illustrated in Figure 1.

Several additional assumptions are made in the model including: (1) negligible vapor holdup in the material and energy balances; (2) perfect mixing in each liquid phase; (3) uniform temperature on each tray; and (4) negligible heat of mixing. These are incorporated in the MESH equations:

Material Balances:

$$\frac{d}{dt}(u_{s,j}) = f^l_{s,j} + f^v_{s,j} + (1-\delta_{Nj})v_{s,j+1} - v_{s,j} + (1-\delta_{1j})l'_{s,j-1} - l'_{s,j} - d'_{s,j} + (1-\delta_{1j})l''_{s,j-1} - l''_{s,j} - d''_{s,j}$$
$$s = 1, \ldots, N_s \text{ and } j = 1, \ldots, N_t \quad (1)$$

Energy Balance:

$$\frac{d}{dt}(E_j) = F^l_j h^F_j + F^v_j H^F_j + (1-\delta_{Nj})V_{j+1}H_{j+1} - V_j H_j + (1-\delta_{1j})L'_{j-1}h'_{j-1} - L'_j h'_j - D'_j h'_j + (1-\delta_{1j})L''_{j-1}h''_{j-1} - L''_j h''_j - D''_j h''_j + Q_j \quad j = 1, \ldots, N_t \quad (2)$$

Vapor-Liquid Equilibrium:

$$K_{s,j}V_j l'_{s,j} - L'_j v_{s,j} = 0$$
$$s = 1, \ldots, N_s \text{ and } j = 1, \ldots, N_t \quad (3a)$$

Liquid-liquid (LL) stage:

$$v_{s,j} = 0 \quad s = 1, \ldots, N_s \text{ and } j = 1, \ldots, N_t \quad (3b)$$

Liquid-Liquid Equilibrium:

$$L_j'' l_{s,j}' \gamma_{s,j}' - L_j' l_{s,j}'' \gamma_{s,j}'' = 0$$
$$s = 1, \ldots, N_s \text{ and } j = 1, \ldots, N_t \quad (4a)$$

Vapor-liquid (VL) stage:

$$l_{s,j}'' = 0 \quad s = 1, \ldots, N_s \text{ and } j = 1, \ldots, N_t \quad (4b)$$

Tray Hydraulics:

$$u_{s,j}^* + \tau_j' l_{s,j}' + \tau_j'' l_{s,j}'' + \tau_j^V v_{s,j} - u_{s,j} = 0$$
$$s = 1, \ldots, N_s \text{ and } j = 1, \ldots, N_t \quad (5)$$

Energy Holdup:

$$E_j - \sum_{s=1}^{N_s} u_{s,j} h_j = 0 \quad j = 1, \ldots, N_t \quad (6)$$

Composition Equalities:

Sidedraw:

$$\frac{d_{s,j}'}{D_j'} = \frac{l_{s,j}'}{L_j'} \quad s = 1, \ldots, N_s \text{ and } j = 1, \ldots, N_t \quad (7)$$

$$\frac{d_{s,j}''}{D_j''} = \frac{l_{s,j}''}{L_j''} \quad s = 1, \ldots, N_s \text{ and } j = 1, \ldots, N_t \quad (8)$$

Summation of Flow Rates:

Vapor Streams:

$$V_j = \sum_s v_{s,j} \quad j = 1, \ldots, N_t \quad (9)$$

Liquid Streams:

$$L_j' = \sum_s l_{s,j}' \quad j = 1, \ldots, N_t \quad (10)$$

$$L_j'' = \sum_s l_{s,j}'' \quad j = 1, \ldots, N_t \quad (11)$$

Feed Streams:

$$F_j^v = \sum_s f_{s,j}^v \quad j = 1, \ldots, N_t \quad (12)$$

$$F_j^l = \sum_s f_{s,j}^l \quad j = 1, \ldots, N_t \quad (13)$$

Reflux Ratios:

$$r_{aq} = \frac{L_1'}{D_1'} \quad (14)$$

$$r_{org} = \frac{L_1''}{D_1''} \quad (15)$$

Note that $u_{s,j}^*$ is the moles of species s on tray j in the liquid holdup when the tower is at rest (zero flow), δ_{ij} is the Kronecker-delta function, and the vapor sidedraws are omitted from the current model.

Specifications and index

Equations 1 to 15 are a system of DAEs containing $N_t(6N_s+7)+2$ equations and $N_t(9N_s+14)+2$ unknowns,

$$(\underline{f}_j^l, \underline{f}_j^v, F_j^l, F_j^v, \underline{u}_j, E_j, \underline{v}_j, V_j, \underline{l}_j', L_j', \underline{d}_j', D_j', T_j, P_j, \underline{l}_j'', L_j'', \underline{d}_j'', D_j'', Q_j, \underline{u}_j^*, \tau_j', \tau_j'', \tau_j^V, r_{aq}, r_{org})^T$$
$$j = 1, \ldots, N_t$$

The $N_t(3N_s+7)$ specifications include the feed streams, and for each stage the pressure (P_j), liquid holdups at zero flow ($\underline{u}_j^*$), and holdup time constants (τ_j', τ_j'', and τ_j^V). In addition, the heat duty (Q_j) for each intermediate tray and the flow rates of the liquid sidedraws (D_j', D_j'') are specified for stages 2 to N_t. With these specifications, four degrees of freedom remain. These are selected among the following variables in the condenser/decanter and the reboiler: condenser duty (Q_1), reboiler duty (Q_{N_t}), aqueous and organic reflux ratios (r_{aq} and r_{org}), aqueous and organic reflux rates (L_1' and L_1''), aqueous and organic distillate rates (D_1' and D_1''), bottoms flow rates (L_{N_t}' and L_{N_t}''), flow rates of the species in the distillate ($d_{s,1}'$ and $d_{s,1}''$), distillate purities ($d_{s,1}'/D_1'$ and $d_{s,1}''/D_1''$), flow rates of the species in the bottoms (d_{N_t}' and d_{N_t}''), and bottoms product purities ($d_{s,N_t}'/D_{N_t}'$ and $d_{s,N_t}''/D_{N_t}''$). In theory, one can specify any four of these variables. Certain combinations, however, result in a high-index system that is unsolvable. To provide an index-1 formulation, the condenser duty (Q_1) and the reboiler duty (Q_{N_t}) must be specified. This is necessary because the differential energy equations (Eq. 2) have state variables E_j and cannot be solved for Q_j, which do not appear in the remaining equations. This, however, can lead to inconsistent specifications and difficulties in obtaining the desired phase distribution in the condenser/decanter. For this reason, unlike Rovaglio and Doherty (1990) and Wong et al. (1991), the phase distribution in the decanter is not specified. It is determined to be VL, LL, or VLL by phase stability analysis. Furthermore, to avoid a high-index formulation, the vapor holdup term cannot be neglected in the tray hydraulics equations. This term is present in most previous formulations (Rovaglio and Doherty, 1990; Ponton and Gawthrop, 1991). Its need to reduce the index is discussed by Widagdo (1991).

Phase stability analysis

The unusual solutions of the MESH equations for heterogeneous azeotropic distillation towers are often closely associated with the transition from one to two liquid phase(s) and are probably due to the quasi-chemical model of the liquid phases. Several observations support this contention. First, for a single stage, multiple solutions are often computed incorrectly for VLE, when the correct solution is LLE (as demonstrated by Van Dongen et al., 1983) or VLLE (as demonstrated by Kingsley and Lucia, 1987). Second, for heterogeneous azeotropic distillation towers, multiple solutions are often computed when all of the stages have a single liquid

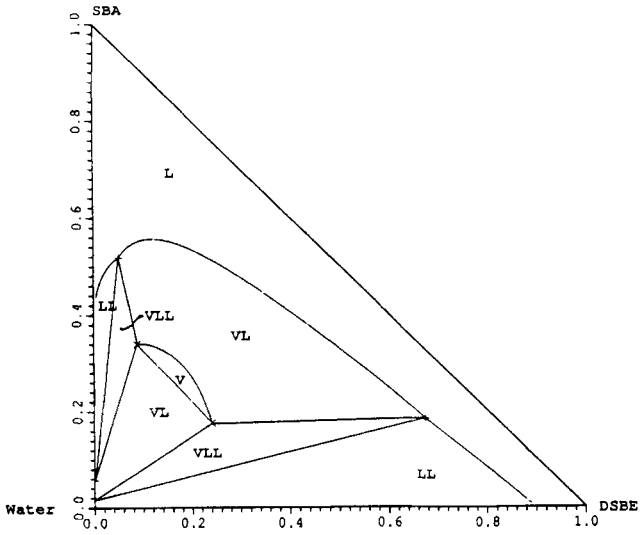

a. Tray 28, at 363.2 K and 1.16996 atm

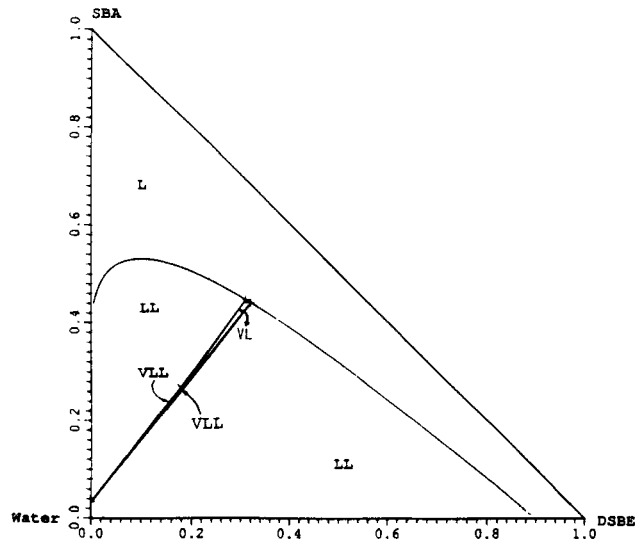

b. Tray 2 (top tray), at 361.5 K and 1.1386 atm

Figure 2. Phase diagrams at conditions of trays 28 and 2 in the steady-state simulation results for a 33-tray tower to dehydrate secbutanol.

phase, but not when some of the stages have two liquid phases (Kovach and Seider, 1987a,b; Kingsley and Lucia, 1988). Widagdo et al. (1989), however, showed the existence of multiple VLE solutions, as a second liquid phase is added to a stage higher in the tower. In addition, heterogeneous azeotropic distillation towers are sensitive to small disturbances, such as small changes in the reflux flow rate. These changes cause the temperature front to shift markedly in the tower. Since the location of this front is often related to the boundary between trays with one and two liquid phase(s), and is commonly measured to control the bottoms purity, it is important to accurately compute the addition and deletion of the second liquid phase. Commonly, however, only the overall liquid phase is tested for instability (Wong et al., 1991), rather than the total contents of the stage (including the vapor phase). By neglecting the vapor phase, it is possible to miss the formation or the deletion of a second liquid phase. Such a test is especially important when the condenser duty is specified and the decanter can have the VL, LL or VLL phase. To obtain more accurate phase distributions, the Gibbs tangent plane criterion, as implemented by Michelsen (1982a,b,c) in the UNIFLASH program, is employed in this work. The phase distribution of each stage and the feed stream is verified at each time step of the integration.

In a companion article (Widagdo et al., 1992), it is shown that due to its two partially-miscible binary pairs and minimum-boiling ternary azeotrope, the secbutanol-water-disecbutylether system has two very narrow VLL regions at the temperatures and pressures approaching its heterogeneous azeotrope. To summarize the results presented therein, Figure 2 provides two phase diagrams at: (a) 363.2 K and 1.16996 atm, the conditions in the steady-state simulation for tray 28 of a 33-tray tower to dehydrate secbutanol; (b) 361.5 K and 1.1386 atm, the conditions on the top tray, tray 2. Near the bottom of the tower, the two VLL regions are far apart and bridged by a sizable vapor envelope. As the heterogeneous ternary azeotrope is approached at the top of the tower, the vapor envelope becomes negligible, separating two thin VLL regions. Hence, to locate the second liquid phase on the top tray, the phase stability test must be implemented very carefully. This is especially important for dynamic simulations where the movement of the interface between trays having one and two liquid phase(s) is very sensitive to small disturbances.

Solution Algorithm

The system of differential/algebraic equations (DAEs, Eqs. 1 to 15) is solved using DASSL (Petzold, 1982). DASSL solves index-1 systems of the form:

$$\begin{aligned} \underline{\mathcal{F}}\{t, \underline{y}, \dot{\underline{y}}\} &= 0 \\ \underline{y}\{t_0\} &= \underline{y}_0 \\ \dot{\underline{y}}\{t_0\} &= \dot{\underline{y}}_0 \end{aligned} \tag{16}$$

where $\underline{\mathcal{F}}$, $\underline{y}$, and $\dot{\underline{y}}$ are N-dimensional vectors. The first derivatives are approximated by the *backward-difference formula* (BDF) of Gear (1971):

$$\dot{y}\{t_n\} \cong \frac{1}{h_n \alpha}\left(y\{t_n\} - \sum_{i=1}^{q} \beta_i y\{t_{n-i}\}\right) \tag{17}$$

where h_n is the step size at $t = t_n$, α and β are constants, and q is the order of the approximation. Substituting Eq. 17 into Eq. 16, the DAEs are transformed into NLEs:

$$\underline{\mathcal{F}}\{t, y, (\hat{\alpha}\underline{y} + \hat{\underline{\beta}})\} = 0 \tag{18}$$

the so-called *corrector* equations. $\hat{\alpha}$ is a constant that depends on the current step size and the order of the BDF. $\hat{\underline{\beta}}$ is a vector of past solutions. These corrector equations are solved by an accelerated Newton's method:

$$\underline{y}\{t_{n+1}\} = \underline{y}\{t_n\} + \Delta\underline{y}\{t_n\} \tag{19}$$

where

$$\Delta \underline{y}\{t_n\} = -C\left(\frac{\partial \underline{\mathcal{F}}}{\partial \underline{y}} + \hat{\alpha}_{n-1}\frac{\partial \underline{\mathcal{F}}}{\partial \dot{\underline{y}}}\right)^{-1} \underline{\mathcal{F}}\{t_n, \underline{y}\{t_n\}, (\hat{\alpha}_n \underline{y}\{t_n\} + \hat{\underline{\beta}})\} \quad (20)$$

with

$$C = \frac{2}{1 + \hat{\alpha}_n/\hat{\alpha}_{n-1}} \quad (21)$$

After successful Newton steps, DASSL computes the local truncation error to determine whether it satisfies the user-supplied tolerances. Once a step is accepted, a new step size and order are computed. Details of the implementation of the backward-difference formula in DASSL are provided by Brenan et al. (1989).

To trace the dynamic response of a heterogeneous separator, several algorithms have been installed in DASSL. These include algorithms for: (1) consistent initialization, (2) the Michelsen phase stability test, and (3) branch switching when the phase distribution changes. In addition, it is necessary to exclude the truncation error estimates of the algebraic variables from the convergence criteria to prevent DASSL from taking unnecessarily small step sizes. To avoid *drifting* of the algebraic variables, an error tolerance is introduced for the algebraic constraints. These latter modifications significantly improve the performance of DASSL in obtaining accurate solutions. The three algorithms are discussed next.

Consistent initialization

When integrating a system of DAEs, it is important to provide consistent initializations prior to starting or restarting the integration. Note that restarts are necessary after the introduction of a disturbance or when the phase distribution changes. In addition to the initial condition for the differential and algebraic variables, DASSL requires initial values for their first derivatives. DASSL provides a general-purpose initialization routine, but unfortunately it has been found by many users to be ineffective. An initialization procedure for index-1 DAEs has been devised and is described next.

Consider a system of implicit, autonomous DAEs:

$$\frac{d\underline{X}}{dt} = \underline{\mathcal{F}}\{\underline{X}, \underline{Y}\} \quad (22a)$$

$$0 = \underline{\mathcal{G}}\{\underline{X}, \underline{Y}\} \quad (22b)$$

where $\underline{X}$ is the vector of differential variables and $\underline{Y}$ is the vector of algebraic variables. Given the initial conditions, $\underline{X}\{t = t_0\} = \underline{X}_0$ and $\underline{Y}\{t = t_0\} = \underline{Y}_0$, the task of finding $\dot{\underline{X}}_0$ and $\dot{\underline{Y}}_0$ can be accomplished by differentiating the system of NLEs with respect to $\underline{X}$ and $\underline{Y}$, resulting in:

$$\begin{bmatrix} \underline{\underline{I}} & \underline{\underline{0}} \\ \underline{\underline{\mathcal{G}}}_X & \underline{\underline{\mathcal{G}}}_Y \end{bmatrix} \begin{bmatrix} \dot{\underline{X}} \\ \dot{\underline{Y}} \end{bmatrix} = \begin{bmatrix} \underline{\mathcal{F}}\{\underline{X}, \underline{Y}\} \\ \underline{0} \end{bmatrix} \quad (23)$$

For index-1 DAEs, the solution of Eq. 23 is guaranteed, since $\underline{\underline{\mathcal{G}}}_Y$ is *nonsingular*. Given $\underline{X}_0$ and $\underline{Y}_0$, Eq. 23 can be solved for $\dot{\underline{X}}_0$ and $\dot{\underline{Y}}_0$. It should be pointed out that although a higher-index formulation may not have a singular integration matrix, a singular $\underline{\underline{\mathcal{G}}}_Y$ prevents consistent initialization. This is not a problem when starting or restarting from a steady state where $\dot{\underline{X}}_0 = \dot{\underline{Y}}_0 = 0$. When a phase is added or deleted during a transient response, however, the inability to reinitialize $\dot{\underline{X}}_0$ and $\dot{\underline{Y}}_0$ causes the integration to be aborted. The initialization algorithm, which has been installed in DASSL, is summarized next.

Algorithm 1:

input:

$\underline{X}_0$ and $\underline{Y}_0$; *initial condition*

Compute the residual, $\underline{\mathcal{F}}\{\underline{X}_0, \underline{Y}_0\}$;

Compute the Jacobian, $\underline{\underline{\mathcal{G}}}_{\alpha X}\{\underline{X}_0, \underline{Y}_0\}$ and $\underline{\underline{\mathcal{G}}}_Y\{\underline{X}_0, \underline{Y}_0\}$;

Solve Eq. 23 for $\dot{\underline{X}}_0$ and $\dot{\underline{Y}}_0$;

Phase stability testing and branch switching

The phase stability test, using the tangent plane criterion (Michelsen, 1982a,b,c), is performed after every successful integration step. This is in contrast to Rovaglio and Doherty (1990), who perform a VLE or VLLE calculation to update the phase distribution when a change in the phase distribution is detected while integrating the MESH DAEs. A similar strategy is used by Wong et al. (1991), in which the instability of the overall liquid is monitored. When instability is detected, a LLE calculation is performed. In both investigations, the new phase distribution is assumed to be stable. Rovaglio and Doherty (1990) acknowledge that this strategy can fail, often resulting in a trivial solution of the VLLE problem. A good initialization of the phase distribution is mandatory, but difficult to provide.

In this work, a novel branch-switching algorithm is proposed. It is based on the intersection of two branches of solutions with different phase distributions at a real bifurcation point, where the two branches intersect transversally, that is, with different slopes. To guarantee that the proper branch is traced, the real bifurcation point must be located. At the real bifurcation point, the phase distribution at equilibrium is computed using the Michelsen algorithm, as implemented in the UNIFLASH program (Michelsen, 1982b,c). Then, the directional tangent vector is computed using the initialization algorithm with the proper phase distribution, determined using the tangent-plane criterion. The integrator is reset, and the new branch is followed. This circumvents convergence to a trivial solution and guarantees smooth branch switching.

In summary, the new algorithm for branch switching is described below.

Algorithm 2:

input:

$\underline{X}\{t_n\}$ and $\underline{Y}\{t_n\}$; *solution from DASSL*

Perform phase stability analysis using the tangent-plane criterion;

If a change in phase distribution is detected **Then**

repeat the integration

Use the half-interval method to locate the real bifurcation point

until convergence;

Table 1. Parameters for UNIQUAC Equation

Size/Shape Parameters	SBA	DSBE	Water	MEK	Butylenes
R	3.9235	6.0909	0.9200	3.2479	2.9209
Q	3.6640	5.1680	1.4000	2.8760	2.5640
Q'	4.0643	5.7409	1.6741	2.8760	2.5640
Interaction Coefficients, $a_{ij}/R\{K\}$					
SBA	0.0000	−97.2021	213.3998	102.5700	−11.4920
DSBE	209.2880	0.0000	158.6873	182.6900	4.8375
Water	52.2446	1,974.0559	0.0000	−0.0386	379.1000
MEK	−32.5860	−57.2900	468.7700	0.0000	−18.1870
Butylenes	162.6000	3.3576	529.5500	107.7600	0.0000

Else
continue the integration;
End If

Algorithm for dynamic simulation of heterogeneous separators

In this section, the complete algorithm for the dynamic simulation of heterogeneous separators is outlined. This algorithm has been implemented in the FORTRAN program, DISDYN.

Algorithm 3:

input:

$\underline{y}_0$ *initial condition*
ϵ_d and ϵ_a; *error tolerances for differential and algebraic subsystems*
h_0; *initial step size*
$k=0$; *integration counter*
t_{end}; *integration limit*
Compute $\dot{\underline{X}}_0$ and $\dot{\underline{Y}}_0$ using Algorithm 1;
repeat
DASSL computes a new solution: $\underline{y}\{t_{k+1}\}$;
Perform phase A stability test;
If phase instability is detected **Then**
activate Algorithm 2;
End If
Compute the phase distribution at equilibrium
(at the real bifurcation point);
Compute the new slope using Algorithm 1;
$k:=k+1$ *advance the integration counter*
until t_{end} is exceeded;

Results

This algorithm has been tested for single- and multistage separators. The SBA-II mixture (secbutanol, disecbutylether, water, methylethylketone, butene-1), a five-component system, is used exclusively in this evaluation. The vapor phase is assumed to be ideal and the liquid phase is modeled using the UNIQUAC equation, with the parameters given in Table 1. Note that the interaction coefficients for the secbutanol-disecbutylether-water system represent the VLE data more accurately than the LLE data. Details of the equilibrium data and the regression analysis are provided by Kovach and Seider (1988).

Table 2. Specifications for the Single-Stage Separator

Feed Flow Rates	
SBA	256.35 kmol/h
MEK	49.80 kmol/h
DSBE	118.81 kmol/h
i-C4	7.57 kmol/h
Water	259.34 kmol/h
Feed Temperature	361.77 K
Feed Pressure	1.2725 atm
Heat Duty	Adiabatic

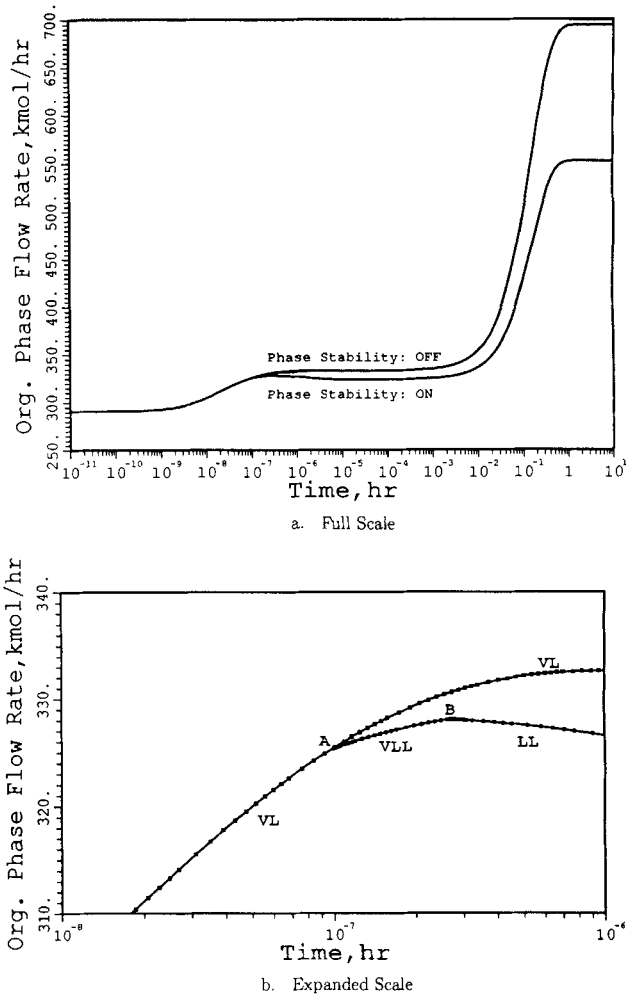

Figure 3. Effect of phase stability analysis on the dynamic response of a cooled VL-separator.

Single-stage separator

To confirm the importance of the phase stability test, a phase separator, into which the SBA-II mixture is fed with specifications in Table 2, is subjected to a 50 kcal/h step decrease in the heat duty. Initially, vapor and liquid phases are separated. The dynamics of the separator are tracked with and without the phase stability test, and their responses are shown in Figure 3a. Note the existence of two different paths. When the phase stability test is off, with the MESH DAEs solved to locate VLL phases, a VL branch is computed. When the phase stability test is on, however, the proper branch is computed, initially VL followed by VLL, as illustrated using a magnified

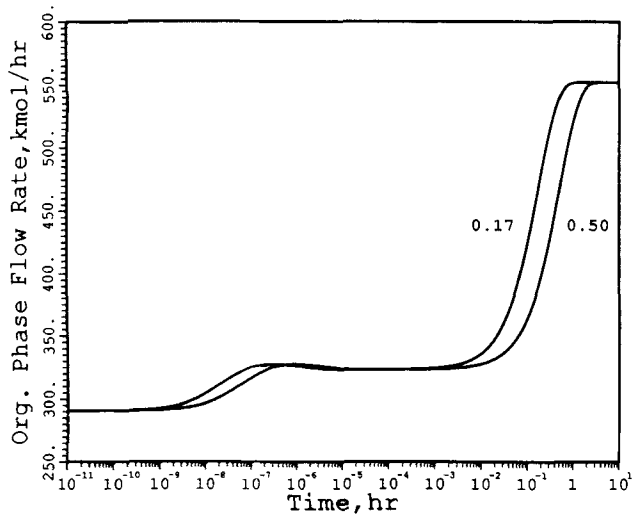

Figure 4. Effect of time constants on the dynamics of a cooled VL-separator.

scale in Figure 3b. To follow the proper branch, it is important to accurately test for phase instability as the integration progresses. In Figure 3b, VL phases are stable to point A. As the temperature decreases, the second liquid phase forms with VLL phases along branch AB. The algorithm correctly locates the VL-VLL transition point A, and the initialization algorithm computes the initial slope of the branch AB. The system temperature further decreases to point B, where the vapor is depleted, leaving stable LL phases. The phase stability algorithm detects this change, and the branch switching algorithm locates point B and computes the initial slope of the LL branch.

Figure 4 shows the effect of the time constants ($\tau' = \tau'' = 0.17$, 0.50 and $\tau^V = 0.017$, 0.050) on the dynamic response of the separator. As expected, the response with larger time constants is more sluggish in its approach to the steady state.

Table 3. Specifications for the 12-Tray Tower

Number of Stages	12
Feed Tray	6
Feed Flow Rates	
SBA	79.92 kmol/h
MEK	0.97 kmol/h
DSBE	1.50 kmol/h
i-C4	0.27 kmol/h
Water	133.26 kmol/h
Feed Temperature	316.48 K
Feed Pressure	1.20 atm
Column Pressure	
Top	1.2725 atm
Bottom	1.29475 atm
Heat Duty	
Stage-1	4.647 Gcal/h
Stage-2 to 11	Adiabatic
Stage-12	4.830 Gcal/h
Reflux Ratios	
Aqueous	0.05
Organic	55.0
Liquid Time Constants ($\tau' = \tau''$)	
Condenser/Decanter	0.17
Stage-2 to 5	0.008
Stage-6 to 11	0.004
Reboiler	0.08
τ^V/τ' *and* τ^V/τ''	0.1

Dehydration of secbutanol with disecbutylether

In this section, the dynamic responses of the SBA-II tower and a shortened 12-tray tower are presented.

12-Tray SBA-II Tower. These simulations begin at the steady state with the specifications in Table 3. Initially, one liquid phase exists on all of the stages, except in the decanter. In all cases, the condenser duty is fixed at its steady-state value.

(1) Changes in the Aqueous Reflux Ratio. At $t = 0$, the aqueous reflux ratio is increased from 0.05 to 0.17 to promote the formation of the second liquid phase. This increase in the reflux is accompanied by an increase in the entrainer concentration in the rectifying section, resulting in higher product purity and recovery. The feed to entrainer ratio decreases, and with the increase in the aqueous reflux a second liquid phase penetrates lower into the rectifying section, shifting the temperature front downward. As illustrated in Figures 5a and 5b, an aqueous phase forms on tray 2 within 5 minutes. Approximately one hour later it has migrated to tray 3, and two hours later to tray 4. After 12 hours a new steady state is achieved, in which four trays with two liquid phases agree with the steady-state results computed by Widagdo et al. (1989). As the aqueous phase penetrates into the rectifying section, the tray temperatures undergo an inverse response before approaching their steady-state values, lower than their initial temperatures. Figure 5c shows a large inverse response for tray temperatures in the rectifying section. Similarly, the temperature front experiences an inverse response, as illustrated in Figure 5d. Throughout this response, the SBA purity in the bottoms product remains acceptable ($\geq 98\%$), as shown in Figure 5e.

(2) Decrease in Reboiler Duty. At $t = 0$, the reboiler duty is decreased by 1 and 2%. With a 1% decrease, no changes in the phase distributions on the stages occur. For a 2% decrease, however, the tower undergoes an underdamped oscillation. Figure 6a shows that within 20 minutes, the aqueous phase penetrates to tray 4. In the next 20 minutes, the aqueous phase disappears from these trays. Then, 30 minutes later, the aqueous phase reappears on tray 2 for about 10 minutes, before leaving the tower as the steady state is approached. The corresponding flow rates of the aqueous phase leaving trays 2 to 4 are shown in Figure 6b.

As illustrated in Figure 6c, the flow rates of the organic phase in the rectifying section respond like a second-order, underdamped system. Wong et al. (1991) observe an inverse response for a tower to dehydrate ethanol, when it is subjected to a 10% increase in the reboiler duty with no changes in the phase distributions. For the SBA-II tower, instead of an inverse response, an underdamped oscillation with a settling time of approximately 5 hours is illustrated in the temperature profiles of Figure 6d. This oscillation accompanies the shifts in the phase distributions on trays 2 to 4. It is observed in the stripping section, but the overshoot and settling time decrease on the trays approaching the reboiler, as illustrated in Figure 6e. Clearly, the impact of the phase pattern changes on trays 2 to 4 have a diminishing effect toward the bottoms of the tower.

The oscillation also appears in the temperature profiles, as illustrated in Figure 6f. Initially, the temperature profile is at *a*, before it moves toward the reboiler. It reverses at *d* and shifts upward to *e*, after which the oscillations are damped as *f* is approached. Hence, the net response is a shift of the temperature front down the tower. The oscillation can be attributed to the following mechanism. The reduction in the

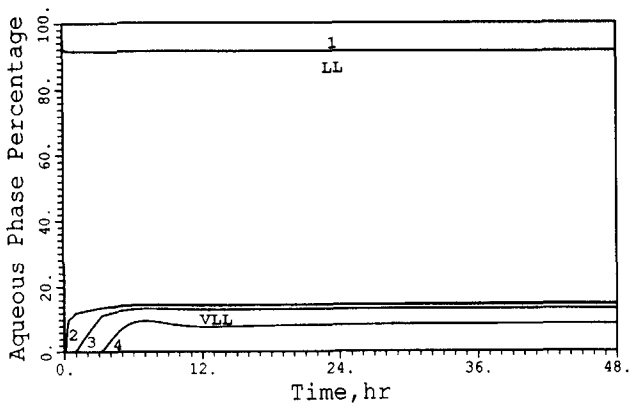

a. Aqueous phase percentage

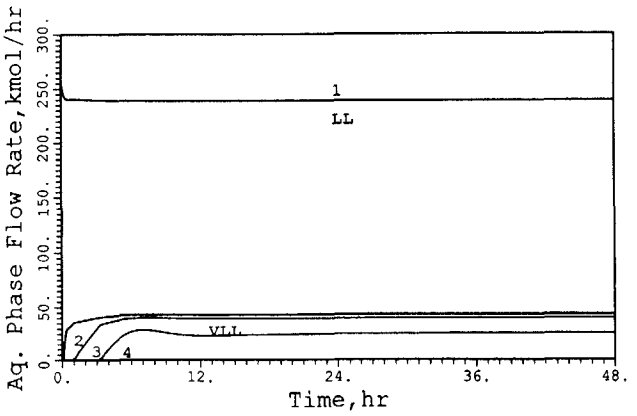

b. Aqueous phase flow rates

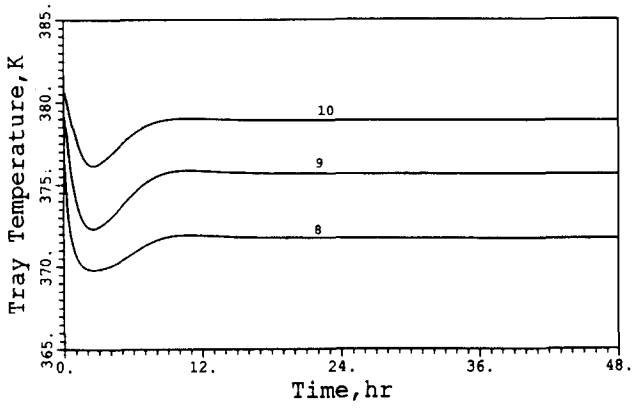

c. Tray temperatures in the rectifying section

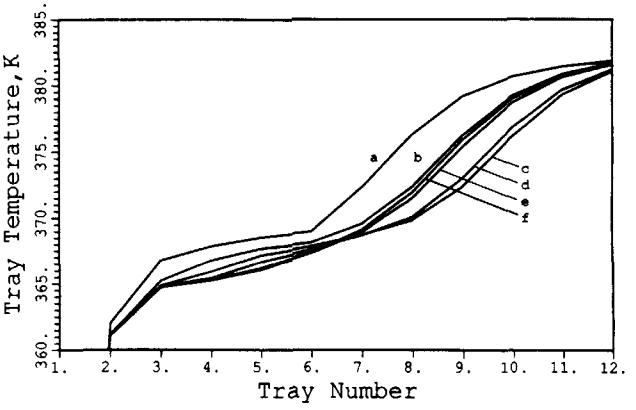

d. Temperature profiles at: (a) $t = 0$, (b) $t = 0.5$, (c) $t = 2.5$, (d) $t = 4.0$, (e) $t = 7.5$, and (f) $t = 10$ hr

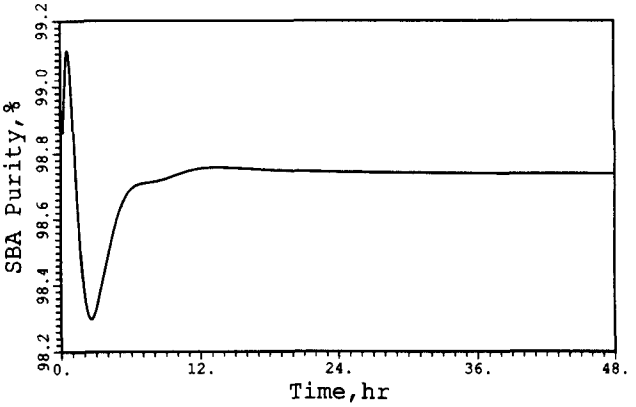

e. SBA purity in the bottoms product

Figure 5. Response of 12-tray tower to a step increase in aqueous reflux ratio from 0.05-0.17. Stage numbers are annotated.

reboiler duty is accompanied by a decrease in the vapor flow rate, which causes the temperatures on the trays to decrease, inducing the formation of a second liquid phase on a few of the trays near the top of the tower. The lower vapor flow rate containing less volatile species increases the feed to entrainer ratio and the temperature front shifts toward the top of the tower, causing the aqueous phase to disappear. As the tray temperatures increase, more volatile species are driven toward the top of the tower, decreasing the feed to entrainer ratio and shifting the temperature front toward the reboiler. This oscillation is repeated with decreasing amplitude, as a new steady state is approached.

Throughout these oscillations, the SBA purity in the bottoms product remains acceptable ($\geq 98\%$), as shown in Figure 6g. These results confirm that the position of the temperature front is an excellent indicator of the bottoms purity. For this reason, it is measured for control purposes.

(3) *Decrease in Feed Flow Rate.* As a final disturbance at $t = 0$, the feed flow rate is decreased by 13%. With the reboiler duty constant, less subcooled feed condenses less vapor in the

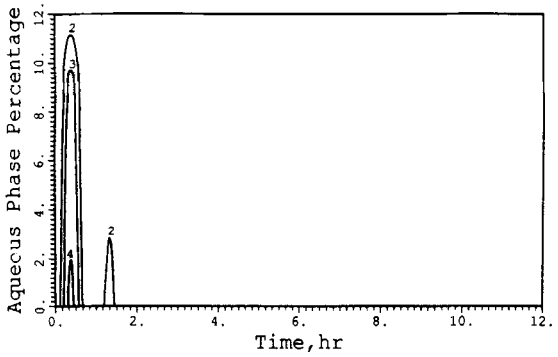

a. Aqueous phase percentage

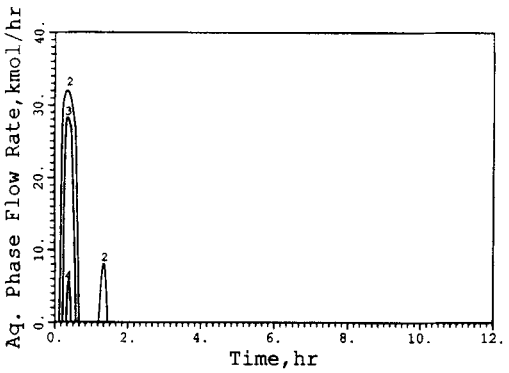

b. Aqueous phase flow rates

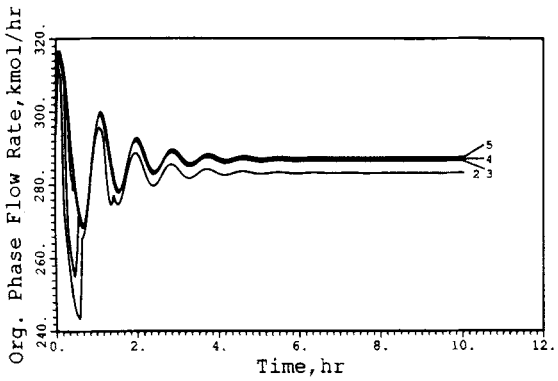

c. Organic phase flow rates in the rectifying section

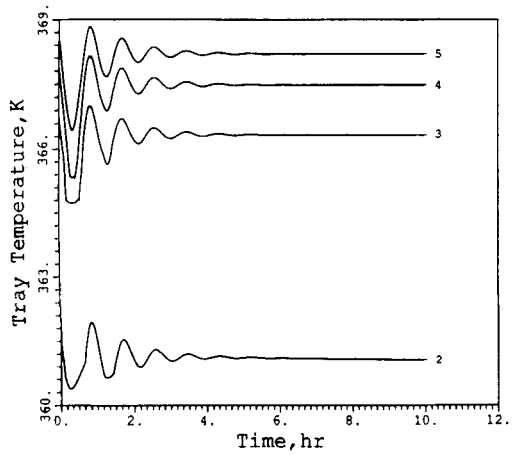

d. Tray temperatures in the rectifying section

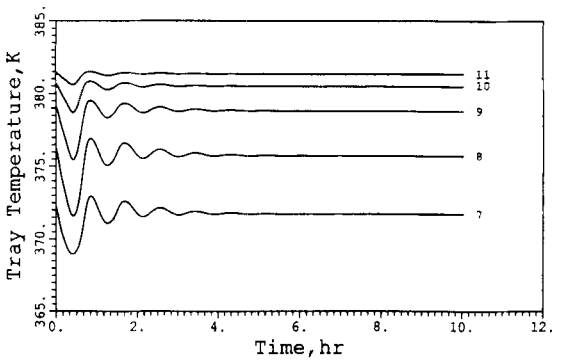

e. Tray temperatures in the stripping section

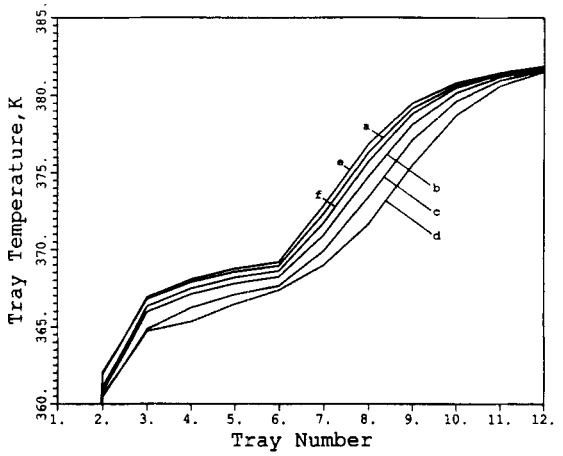

f. Temperature profiles at: (a) $t = 0$, (b) $t = 0.1$, (c) $t = 0.2$, (d) $t = 0.4$, (e) $t = 0.8$, and (f) $t = 10$ hr

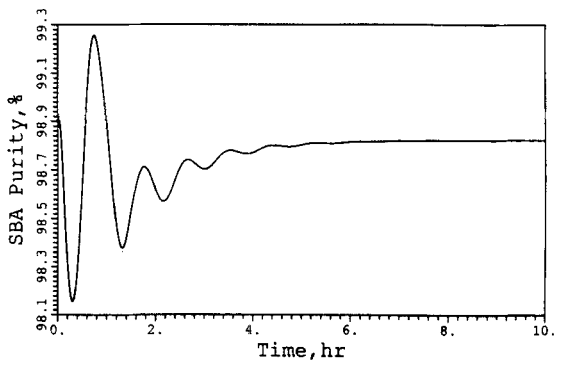

g. SBA purity in the bottoms product

Figure 6. Response of 12-tray tower to 2% decrease in reboiler duty. Stage numbers are annotated.

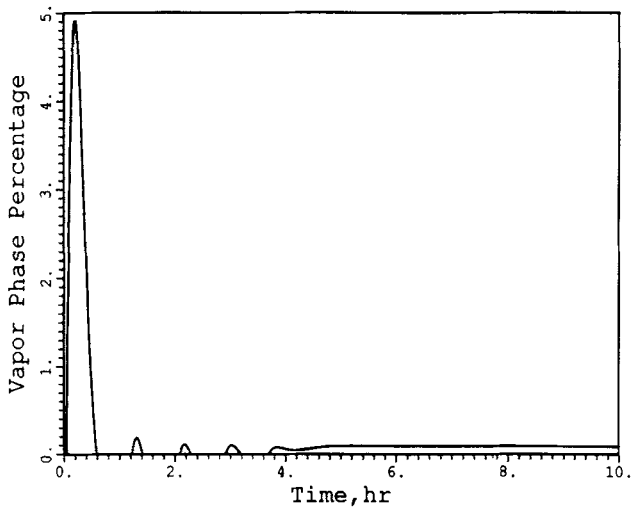

a. Vapor phase percentage in the decanter

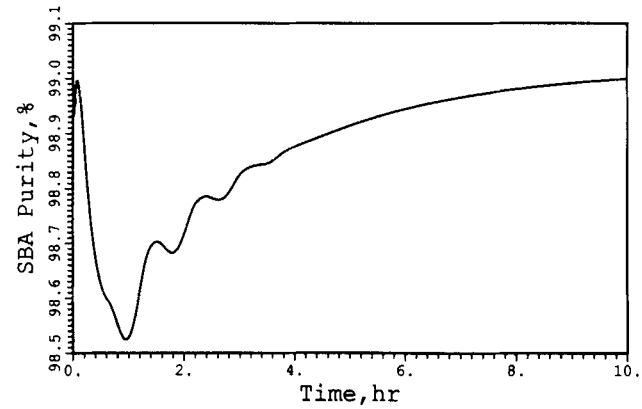

b. SBA purity in the bottoms product

Figure 7. Response of 12-tray tower to 13% decrease in the feed flow rate.

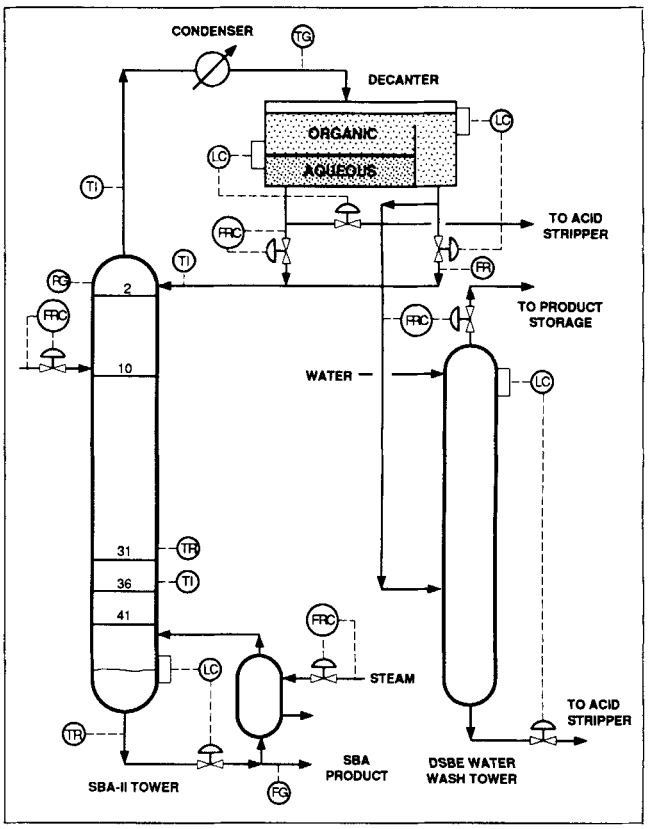

Figure 8. PID for the SBA-II distillation tower.

stripping section and the overhead vapor increases. With a constant cooling rate, the overhead vapor is not condensed entirely and vapor appears in the decanter. Subsequently, since the feed to entrainer ratio decreases, the temperature front shifts downward, the rectifying section cools, and the vapor phase disappears in the decanter. These effects are repeated, but with far less vapor leaving the condenser. After approximately 5 hours, a steady state is approached with a small amount of vapor leaving the condenser, as illustrated in Figure 7a. As shown in Figure 7b, the changes in the phase distribution cause the secbutanol purity to oscillate, followed by a slow movement toward the new steady state.

(4) Computation Time. All of the calculations were performed on the VAX-8700 computer with an average of 10 CPU min for one hour of real time.

SBA-II Tower. Before describing the simulation results, the ARCO SBA-II tower is reviewed briefly. See Kovach and Seider (1987a) for a more complete description of the tower and the experimental measurements.

A process instrumentation diagram (PID) for the SBA-II tower is presented in Figure 8. The tower has 39 valve trays and a large decanter (1.829 m ID, 8.23 m TT) with a 40- to 50-min residence time for the combined aqueous and organic phases. Heat is supplied by a 175.1-m^2 thermo-siphon reboiler and removed by a 319.6-m^2 condenser. Under normal operating conditions, the reboiler and condenser duties are 4.83 and 4.62 Gcal/h, respectively.

The temperature of tray 31 is recorded continuously, while temperature indicators are used for tray 36, the overhead vapor and the reflux streams. The flow rates of the feed, organic product, aqueous reflux and the steam rate are controlled with flow-rate recorder controllers (FRC). The aqueous product rate and the organic reflux rate are controlled by level controllers and monitored by flow recorders. The bottoms flow rate is adjusted by a level controller.

The main control objective is to maintain the purity of secbutanol in the bottoms above 98 wt. %. The control strategy is to maintain the water to entrainer ratio such that the temperature difference between trays 31 and 36 is about 8 K. Due to the sensitivity of the response, this is accomplished by adjusting the flow rate of the aqueous reflux manually.

In normal operation, the feed and reboiler steam rates vary between 1 to 5%. The operator adjusts the aqueous reflux rate to position the temperature front between trays 31 and 36. The secbutanol purity is closely related to the position of this front, and therefore its position is monitored to achieve the desired purity.

(1) Experimental Dynamics Test. Kovach (1986) reports the results of a dynamics test for the SBA-II tower. Before the test, steady operation was not observed. Many process variables fluctuated while others remained constant. Neither the steam nor the feed rates varied more than 5% in the three days

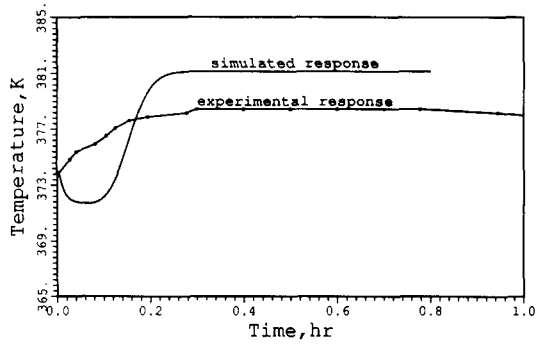

a. Experimental T_{31} and simulated T_{26}

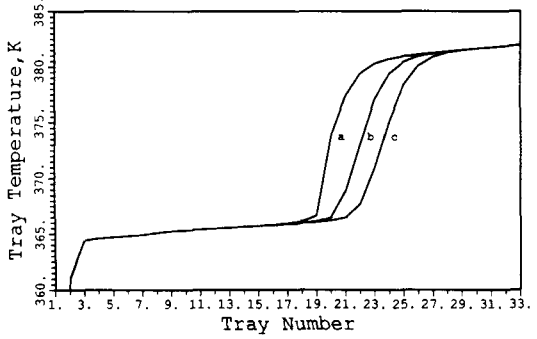

b. Temperature profiles at aqueous reflux rates: (a) 3.3, (b) 4.5, and (c) 5.75 gpm

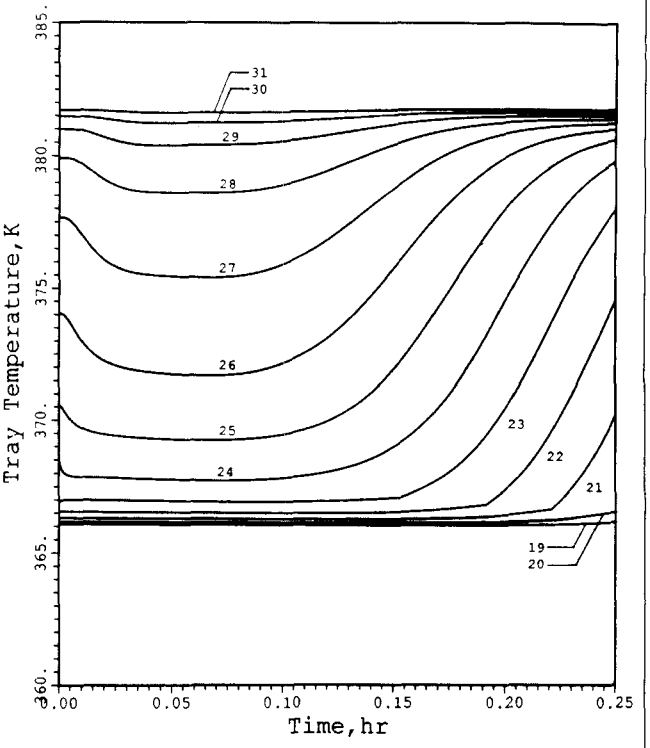

c. Temperatures of trays in the stripping section with an aqueous reflux rate of 3.3 gpm

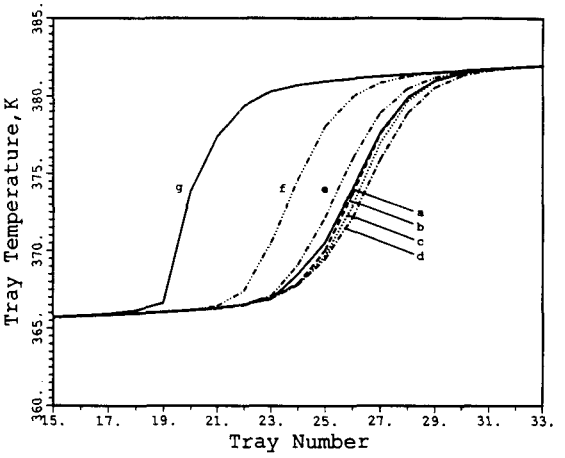

d. Temperature profiles at: (a) $t = 0$, (b) $t = 0.3$, (c) $t = 0.6$, (d) $t = 6.0$, (e) $t = 9.0$, (f) $t = 12.0$, and (g) $t = 17.0$ min. Aqueous reflux rate is 3.3 gpm

Figure 9. Response of the SBA-II tower to a 13% decrease in the feed flow rate.

preceding the dynamic test. The aqueous reflux rate varied about 1.6 gpm ($\sim \pm 0.16$ gpm) [0.1 L/s ($\sim \pm 0.01$ L/s)]. This translates to an aqueous reflux ratio of 0.153, closer to the results herein than that reported by Kovach and Seider (1987a). Note that the latter results were computed inadvertently with $\Delta T_{sc} = 50$ K (rather than 1 K, as reported in the manuscript). This led to a sizable error in the decanter temperature and a low aqueous reflux ratio.

The test began at 08:10 with a 13% decrease in the feed flow rate from 41.4 to 36.0 gpm (2.6 to 2.3 L/s). This reduction decreased the water to entrainer ratio and shifted the temperature front up the tower. To counteract this shift, the aqueous reflux rate was increased simultaneously from 1.6 to 2.8 gpm (0.1 to 0.18 L/s). As illustrated in Figure 9a, within 30 minutes, the temperature on tray 31, T_{31}, increased rapidly to 378.2 K. The aqueous reflux was increased further reaching a maximum of 3.3 gpm (0.21 L/s) at 09:05. By this time, the movement of the front was reversing and the aqueous reflux was held constant for another 10–15 minutes.

(2) Simulated Dynamic Test. The tower is simulated with 33 trays, assuming an overall efficiency of 80%, and the simulation begins at steady state, with the specifications in Table

Table 4. Specifications for the 33-Tray Tower

Number of Stages	33
Feed Tray	8
Feed Flow Rates	
SBA	79.92 kmol/h
MEK	0.97 kmol/h
DSBE	1.50 kmol/h
i-C4	0.27 kmol/h
Water	133.26 kmol/h
Feed Temperature	316.48 K
Feed Pressure	1.20 atm
Column Pressure	
Top	1.2725 atm
Bottom	1.3949 atm
Heat Duty	
Stage-1	4.62 Gcal/h
Stage-2 to 32	Adiabatic
Stage-33	4.83 Gcal/h
Reflux Ratios	
Aqueous	0.177658
Organic	55.0
Liquid Time Constants ($\tau' = \tau''$)	
Condenser/Decanter	0.17
Stage-2 to 7	0.008
Stage-8 to 31	0.004
Reboiler	0.08
τ^V/τ' *and* τ^V/τ''	0.1

4. This corresponds to an aqueous reflux ratio of 0.177658, organic reflux ratio of 55, reboiler duty of 4.83 Gcal/h, and two liquid phases on 23 trays. To simulate temperature control in the condenser, the condenser duty is adjusted in proportion to the overhead vapor flow rate. Instead of specifying the aqueous reflux ratio, the aqueous reflux rate is adjusted to 41.635 kmol/h [3.3 gpm (0.21 L/s)].

The decrease of 13% in the feed flow rate reduces the supply of water by 17.324 kmol/h [1.373 gpm (0.0866 L/s)]. As the water/entrainer ratio decreases, the temperature front is expected to move up the tower. To maintain the position of the front, the aqueous reflux rate is increased from 1.6 gpm (0.1 L/s) to 3.3 gpm (0.21 L/s) in a single step. Since the aqueous reflux is introduced at the top of the tower and secbutanol in the feed is reduced, both the experimental and the simulation results show that the temperature front shifts upward, as illustrated in Figure 9a. Furthermore, the simulation predicts that the steady-state temperature on tray 26 (tray 31 in the SBA-II tower) is 2.5 K higher than the experimental measurements. Hence, the simulated temperature front is higher in the tower, suggesting that a higher aqueous reflux rate might provide a better match with the data. Simulation results for three aqueous reflux rates [3.3, 4.5 and 5.75 gpm (0.21, 0.28 and 0.36 L/s)] are shown in Figure 9b. Unfortunately, the temperature of tray 26 does not vary significantly with the aqueous reflux ratio, and hence the simulation results cannot be improved with small increases in the aqueous reflux rate. This may be explained by the inability of the model to accurately represent the VLLE data.

The temperatures of trays in the stripping section for an aqueous reflux rate of 3.3 gpm (0.21 L/s) are shown in Figure 9c. Note that the trays with two liquid phases (<23) do not exhibit the inverse response displayed on trays with a single liquid phase (>23). The inverse response occurs after the reduction in the feed flow rate which increases the entrainer/feed ratio and initially shifts the temperature front downward. The experimental results do not exhibit this inverse response, possibly due to the unmeasured actions of controllers that are not included in the simulation. Nine minutes later the second liquid phases coalesces on tray 23, due to the reduction of water fed to the tower and the temperature front shifts upward, as illustrated in Figure 9d.

The discrepancy in the rate of change of the temperature on tray 26 may be due to the failure of the model to accurately represent the tray hydraulics.

Approximately three hours of VAX-8700 CPU time were required to simulate 0.8 h of real time. For this simulation involving 33-trays, a faster machine is necessary for real-time control. Recent workstations are almost ten times faster and should be adequate for this purpose.

In summary, although quantitative agreement is not obtained, the results are in qualitative agreement. Despite the inability to duplicate the exact conditions of the dynamic test, such as the responses of the level controllers in the decanter and in the bottoms of the tower, the simulated results appear to be satisfactory for control purposes. The discrepancies between the experimental and simulation results are not clear, but may be due to the inability of the model to accurately represent the tray hydraulics and the VLLE data.

Conclusion

In previous studies, complex nonlinear effects in the heterogeneous azeotropic distillation towers have been discovered through steady-state simulation. This work extends these studies and introduces a more rigorous model and algorithm for the dynamic simulation of these towers. The model and algorithm are particularly effective for the separation of mixtures involving two partially-miscible binary pairs, as it occurs in the dehydration of secbutanol with disecbutylether.

More specifically, the conclusions are:

- A general and reliable algorithm for simulating the dynamics of heterogeneous azeotropic distillation has been developed. Included are an algorithm for the consistent initialization of index-1 DAEs, a novel algorithm for branch switching when the phase distribution changes at a real bifurcation point, and a more effective algorithm for phase stability analysis. This algorithm has been implemented in a FORTRAN 77 program, DISDYN.
- The proposed algorithm offers a reliable, consistent initialization for index-1 DAEs. Unlike prior algorithms, the integration can be started and restarted with initial conditions other than at a steady state. Thus, the algorithm is well suited for dynamic simulations with multiple disturbances and phase changes, after which the DAE solver must be restarted.
- A reliable branch-switching algorithm has been developed to locate the intersection of two branches with different phase distributions at a real bifurcation point: First, the bifurcation point is located; second, the slope of the new branch is computed. This strategy at the interface between trays having VL and VLL phases circumvents convergence to the VL solution, when VLL phases exist at equilibrium, a potential drawback of the Rovaglio and Doherty (1990) and Wong et al. (1991) algorithms.
- Combined with a more effective phase stability analysis, using the tangent-plane criterion, as implemented by Michelsen (1982a,b,c), the proposed algorithm has superior performance.

The test cases show great promise for more reliable dynamic simulations of heterogeneous azeotropic distillation towers.

- The open-loop response of a shortened SBA-II tower has been studied extensively. In all cases, the program performs well in tracing the proper branch as the integration proceeds. The 12-tray tower is more sensitive to changes in the reboiler duty as compared to changes in the reflux ratio. Since the location of the temperature front is closely related to the sec-butanol purity, it can be measured to control the product concentration. Furthermore, the response times for the shortened tower are sufficiently long to suggest the effectiveness of model-predictive controllers.
- Although quantitative agreement is not obtained, the comparison with the dynamic test conducted on the SBA-II tower is in qualitative agreement.

Acknowledgment

The authors would like to express their gratitude to Linda Petzold of the Lawrence Livermore Laboratory for fruitful discussions on the use of DASSL and for providing the materials in her book prior to publication. The generosity of Michael L. Michelsen, Instituttet for Kemiteknik, Danmarks Tekniske Hojskole, in providing the UNIFLASH program is gratefully acknowledged. The helpful comments of Joseph W. Kovach, III, are appreciated. Partial funding was provided by the Design Theory and Methodology Program of the NSF under grant no. DMC-8613484 and is gratefully acknowledged.

Notation

C = asymptotic convergence constant
d_s = sidedraw flow rate of species s, kmol/h
D = total sidedraw flow rate leaving tray j, kmol/h
E_j = energy holdup on tray j, kcal
f = vector of species flow rates in the feed stream, kmol/h
F_j = total feed rate to tray j, kmol/h
$\underline{\mathfrak{F}}$ = vector of the residuals of the differential equations
$\underline{\underline{G}}_X$ = matrix of the partial derivatives of the nonlinear equations with respect to the *differential* variables
$\underline{\underline{G}}_Y$ = matrix of the partial derivatives of the nonlinear equations with respect to the *algebraic* variables
$\underline{G}$ = vector of the residuals of the nonlinear equations
h_j = enthalpy of the liquid phase on tray j
h_n = integration step length at $t=t_n$
h_0 = initial integration step length
H_j = enthalpy of the vapor phase on tray j
$K_{s,j}$ = vapor-liquid equilibrium constant of species s on tray j
l = vector of species liquid flow rates, kmol/h
L_j = total flow rate leaving tray j, kmol/h
N_s = number of chemical species
N_t = total number of the equilibrium stages
P_j = pressure on tray j
q = order of the approximation in the backward difference formula
Q_j = rate of heat transfer to tray j, kcal/h
r_{aq} = aqueous reflux ratio
r_{org} = organic reflux ratio
t = time
t_{end} = integration limit
T_j = temperature on tray j
ΔT_{sc} = degree of subcooling in the condenser/decanter, K
u = vector of species liquid holdups, kmol
u_j^* = vector of species liquid holdups at rest on tray j, kmol
v = vector of species vapor flow rates, kmol/h
V_j = total vapor flow rate leaving tray j, kmol/h
$\underline{X}$ = vector of differential variables
$\underline{Y}$ = vector of *algebraic* variables

Greek letters

$\alpha, \hat{\alpha}$ = constants in the backward difference formula
$\beta_i, \hat{\beta}_i$ = ith constants in the backward difference formula
γ_s = activity coefficient of species s in the liquid phase
δ_{ij} = Kronecker-delta function
τ = residence time, h

Subscripts

aq = aqueous phase
j = tray index
n = integration index
org = organic phase
s = species index
0 = initial value

Superscripts

f, F = feed stream
l, L = liquid phase
v, V = vapor phase
$'$ = first liquid phase
$''$ = second liquid phase

Literature Cited

Baden, N., and M. L. Michelsen, "Computer Methods for Steady-State Simulation of Distillation Columns," *Inst. Chem. Eng. Symp. Ser.*, **104**, 425 (1987).

Ballard, D. M., and C. B. Brosilow, "Dynamic Simulation of Multicomponent Distillation Columns," AIChE Meeting, Miami (1978).

Block, U., and B. Hegner, "Development and Application of A Simulation Model for Three-Phase Distillation," *AIChE J.*, **22**, 582 (1976).

Brenan, K. E., S. L. Campbell, and L. R. Petzold, *Numerical Solution of Initial-Value Problems in Differential-Algebraic Equations*, North-Holland, New York (1989).

Cairns, B. P., and I. A. Furzer, "Multicomponent Three Phase Azeotropic Distillation: 1. Extensive Experimental Data and Simulation Results," *Ind. Eng. Chem. Res.*, **29**, 1349 (1990).

Ferraris, G. B., and M. Morbidelli, "Mathematical Modeling of Multistaged Separators with Mixtures Whose Components Have Largely Different Volatilities," *Comput. Chem. Eng.*, **6**, 4, 303 (1981).

Gear, C. W., "Simultaneous Numerical Solution of Differential/algebraic Equations," *IEEE Trans. Circ. Theo.*, **CT-18**, 89 (1971).

Herron, Jr., C. C., B. K. Kruelskie, and J. R. Fair, "Hydrodynamics and Mass Transfer on Three-Phase Distillation Trays," *AIChE J.*, **34**, 1267 (1988).

Kingsley, J. P., and A. Lucia, "Simulation and Optimization of Three-Phase Distillation Processes," AIChE Meeting, Houston (1987).

Kingsley, J. P., and A. Lucia, "Simulation and Optimization of Three-Phase Distillation Processes," *Ind. Eng. Chem. Res.*, **27**, 1900 (1988).

Kovach III, J. W., "Heterogeneous Azeotropic Distillation—An Experimental and Theoretical Study," PhD Thesis, Univ. of Pennsylvania (1986).

Kovach, III, J. W., and W. D. Seider, "Heterogeneous Azeotropic Distillation: Experimental and Simulation Results," *AIChE J.*, **33**(8), 1300 (1987a).

Kovach, III, J. W., and W. D. Seider, "Heterogeneous Azeotropic Distillation: Homotopy-continuation Methods," *Comput. Chem. Eng.*, **11**(6), 593 (1987b).

Kovach III, J. W., and W. D. Seider, "Vapor-Liquid and Liquid-Liquid Equilibria for the System sec-Butyl Alcohol-Di-sec-butyl-Ether-Water," *J. Chem. Eng. Data*, **32**, 16 (1988).

Michelsen, M. L., "The Isothermal Flash Problem: I. Stability," *Fluid Phase Equil.*, **9**, 1 (1982a).

Michelsen, M. L., "The Isothermal Flash Problem: II. Phase Split Calculation," *Fluid Phase Equil.*, **9**, 21 (1982b).

Michelsen, M. L., *Phase Equilibria and Separation Processes: Manual for UNIFLASH*, Instituttet for Kemiteknik, Danmarks Tekniske Hojskole, Lyngby, Denmark (1982c).

Naphtali, L. M., and D. P. Sandholm, "Multicomponent Separation Calculations by Linearization," *AIChE J.*, **17**, 148 (1971).
Petzold, L. R., "A Description of DASSL: A Differential/Algebraic System Solver," Sandia Report, SAND82-8637 (1982).
Ponton, J. W., and P. J. Gawthrop, "Systematic Construction of Dynamic Models for Phase Equilibrium Processes," *Comput. Chem. Eng.*, **15**, 12, 803 (1991).
Prokopakis, G. J., and W. D. Seider, "Dynamic Simulation of Azeotropic Distillation Towers," *AIChE J.*, **29**(6), 1017 (1983).
Ross, B. A., and W. D. Seider, "Simulation of Three-Phase Distillation Towers," *Comput. Chem. Eng.*, **5**, 7 (1980).
Rovaglio, M., and M. F. Doherty, "Dynamics of Heterogeneous Distillation Columns," *AIChE J.*, **36**, 39 (1990).
Swartz, C. L. E., and W. E. Stewart, "Finite-Element Steady State Simulation of Multiphase Distillation," *AIChE J.*, **33**, 1977 (1987).
Van Dongen, D. B., M. F. Doherty and J. R. Haight, "Material Stability of Multicomponent Mixtures and the Multiplicity of Solutions to Phase-equilibrium Equations: 1. Nonreacting Mixtures," *Ind. Eng. Chem. Fund.*, **22**, 472 (1983).
Widagdo, S., "Dynamic Analysis of Heterogeneous Azeotropic Distillation," PhD Thesis, Stevens Inst. of Technol. (1991).
Widagdo, S., W. D. Seider, and D. H. Sebastian, "Bifurcation Analysis in Heterogeneous Azeotropic Distillation," *AIChE J.*, **35**(9), 1457 (1989).
Widagdo, S., W. D. Seider, and D. H. Sebastian, "Phase Equilibria for Heterogeneous Azeotropes with Two Partially-miscible Binary Pairs," *Fluid Phase Equil.*, submitted (1992).
Wong, D. S. H., S. S. Jang, and C. F. Chang, "Simulation of Dynamics and Phase Pattern Changes for an Azeotropic Distillation Column," *Comput. Chem. Eng.*, **15**(5), 325 (1991).

Manuscript received Feb. 10, 1992, and revision received May 29, 1992.